

MIT Open Access Articles

*Distribution of Thermally Activated
Plastic Events in a Flowing Glass*

The MIT Faculty has made this article openly available. **Please share** how this access benefits you. Your story matters.

Citation: Rodney, David , and Christopher Schuh. "Distribution of Thermally Activated Plastic Events in a Flowing Glass." *Physical Review Letters* 102.23 (2009): 235503. (C) 2010 The American Physical Society.

As Published: <http://dx.doi.org/10.1103/PhysRevLett.102.235503>

Publisher: American Physical Society

Persistent URL: <http://hdl.handle.net/1721.1/51337>

Version: Final published version: final published article, as it appeared in a journal, conference proceedings, or other formally published context

Terms of Use: Article is made available in accordance with the publisher's policy and may be subject to US copyright law. Please refer to the publisher's site for terms of use.



Distribution of Thermally Activated Plastic Events in a Flowing Glass

David Rodney* and Christopher Schuh

Department of Materials Science and Engineering, Massachusetts Institute of Technology, Cambridge, Massachusetts 02139, USA
(Received 23 January 2009; published 12 June 2009)

The potential energy landscape of a flowing metallic glass is revealed using the activation-relaxation technique. For a two-dimensional Lennard-Jones system initially deformed into a steady-state condition through quasistatic shear, the distribution of activation energies is shown to contain a large fraction of low-energy barriers, consistent with a highly nonequilibrium flow state. The distribution of plastic strains has a fundamentally different shape than that obtained during quasistatic simulations, exhibiting a peak at finite strain and, after elastic unloading, a nonzero mean plastic strain that evidences a polarization of the flow state. No significant correlation is found between the activation energy of a plastic event and its associated plastic strain.

DOI: 10.1103/PhysRevLett.102.235503

PACS numbers: 62.20.F-, 61.43.Dg

The plasticity of metallic glasses is a field of very active research [1], relevant for the broader class of disordered solids that includes covalent glasses [2] and fibrous materials [3]. The current challenges in this field are both technological, related to the need of improving the mechanical reliability of metallic glasses and avoiding strain localization [4,5], and fundamental, directed at the development of a consistent theory of plastic deformation [6,7] similar to the dislocation theory of crystals.

Atomic-scale computer simulations have played a central role in this field since the pioneering works of Kobayashi, Maeda, and Takeuchi [8] and Deng, Argon, and Yip [9]. Conceptual progress has been made recently by application of the inherent structure formalism [10] to disordered systems under quasistatic conditions of deformation [11]. When a glass is strained incrementally with full relaxation between increments, its deformation proceeds by a succession of reversible elastic branches in which the system remains in a given inherent structure, i.e., a local minimum of the potential energy landscape. Punctuating these elastic branches are plastic events that occur when a position of instability is reached and the system irreversibly transitions to a new inherent structure. Through these plastic transitions the glass reaches a steady flow state, traversing a succession of high-energy inherent structures [2]. In two-dimensional simulations of this kind, the unit plastic events have been identified as shear transformation zones [6,12], with localized quadrupolar rearrangements [13,14]. It has also been shown that during a single plastic transition an initial shear transformation zone may trigger a cascade of rearrangements that percolate through the simulation cell [13,15].

It is important to note that the works summarized above, like the majority of simulations conducted on amorphous systems, are performed in athermal conditions. In any given inherent state, there is a distribution of saddle points that correspond to different possible plastic events. In an athermal simulation, the glass can leave its current inherent

structure only through the first barrier to vanish as the stress increases. On the other hand, at finite temperature, the entire distribution of possible events is accessible through thermal fluctuations. We expect, therefore, that the succession of plastic transitions undergone during a quasistatic or athermal simulation is not representative of the distribution of events available in the energy landscape.

Our purpose in this Letter is to identify the distributions of activated plastic events in a deforming amorphous system. We therefore employ a static approach and study thermal activation through the influence of plastic deformation on the potential energy landscape of a glass. The results presented here are thus relevant for low temperatures where the transition state theory can be applied. Although recent atomic-scale simulations have used excitation methods [16,17] to assess the average activation energies for flow, the present study is intended to be the first direct determination of plastic event distributions in the flow state, including the activation energy spectrum and the associated plastic strains. We adopt the activation-relaxation technique (ART nouveau) of Malek and Mousseau [18], which has been used successfully to study diffusion in amorphous silicon [19], with an improved saddle-point convergence algorithm [20]. We explore the potential energy landscape of a highly driven metallic glass—one deformed to the steady state through quasistatic shear deformation—and evaluate how the plastic event distributions are affected during elastic unloading, i.e., at various applied stress levels.

We consider a model $\text{Cu}_{50}\text{Zr}_{50}$ metallic glass in two dimensions, made of 4000 atoms interacting through Lennard-Jones potentials [8,9]. The amorphous structure was quenched at a rate of 10^{11} K/s from a low-density gas and initially has zero average internal stresses. A portion of a typical configuration is shown in Fig. 1. A shear stress $\tau = \sigma_{XY}$ is effected by imposing a shear strain γ_{XY} through Lees-Edwards [21] shifted periodic boundary conditions. We first simulate quasistatic shear deformation up

to 200% strain, through the application of strain increments of 10^{-4} followed by conjugate gradient minimizations, as in Refs. [13,14]. We then extract equilibrium configurations at different applied strains and unload them quasistatically by decreasing the applied strain until the average shear stress is zero. These unloadings occasionally involve plastic events but are mostly elastic, such that the system can be considered to have remained in the same inherent structure. Several configurations unloaded to different average shear stresses are subsequently used as initial configurations in ART. Distributions from different unloadings show some scatter but follow the same trends we report below, confirming that we analyze the steady-state flow state.

The ART nouveau method is used to find activated states. It is an eigenvector-following method in which the direction of minimum curvature is obtained iteratively using the Lanczos algorithm [18,20]. The initial equilibrium configuration is first pushed out of its basin along a random direction in configuration space with a fixed step length of 5×10^{-2} nm. In order to account for the localized nature of thermal excitations, we choose the initial direction as a random displacement of a randomly chosen atom. After the displacement, 5 relaxation steps are taken perpendicularly to the direction of motion in order to avoid a rapid rise of the system energy. Fixed-length displacements are iterated until the curvature becomes negative and less than -1 eV/nm². The system is then relaxed to a saddle point, by following the same procedure as above but using the variable step length proposed by Cancès *et al* [20] (with no cutoff in eigenvalue but a maximum step length of 0.01 nm) and maintaining the direction of motion along that of maximum negative curvature through 15

Lanczos iterations per step. The search is stopped if the curvature becomes positive again, in which case a new search is started. The saddle point is considered reached if the maximum atomic force component is less than 10^{-3} eV/nm. The saddle-point configuration is then perturbed along the direction of negative curvature, both towards and away from the initial configuration, in order to ensure that the saddle point is still connected to the initial configuration and to obtain the final configuration. The activation energy is then the difference in energy between the initial and activated configurations, while the plastic strain is given by $\gamma_P = -\Delta\tau/\mu$ where $\Delta\tau$ is the difference in shear stress between final and initial configurations and μ is the shear modulus computed from the slope of the quasistatic elastic branches. For each initial state, 4000 different activated events were determined; i.e., redundant saddles were not accounted for. This is a small fraction of the total number of saddles, and ART is known to be biased towards low-energy barriers [19]. Larger samples would contain a larger fraction of high-energy events. However, the sample size used here is large enough to capture the shape of the distributions and the physical effects associated with them.

An example of an activated state is presented in Fig. 1. Most activated configurations are localized, as in Fig. 1. (This is in contrast with final states, a significant fraction of which exhibit displacement cascades that percolate through the simulation cell; we will return to this point at the end of the Letter.) Activated states can have different morphologies: very few exhibit the pronounced quadrupolar symmetry characteristic of shear transformation zones found in quasistatic simulations [13,14] and in some final

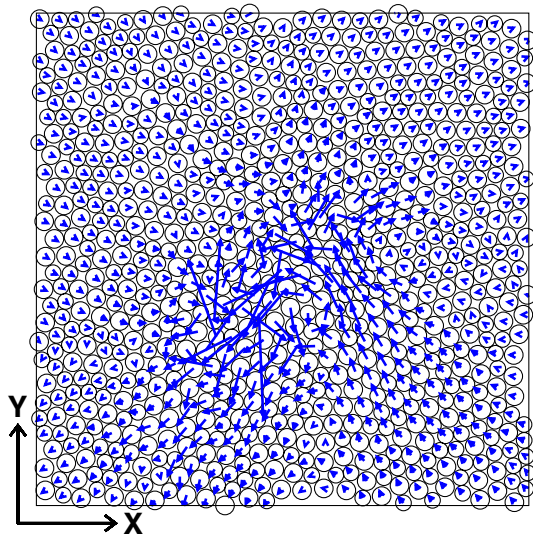


FIG. 1 (color online). Example of an activated plastic event. Arrows show the atomic displacements between an initial and an activated configuration (magnification factor 7). Only a section of the simulation cell is shown here.

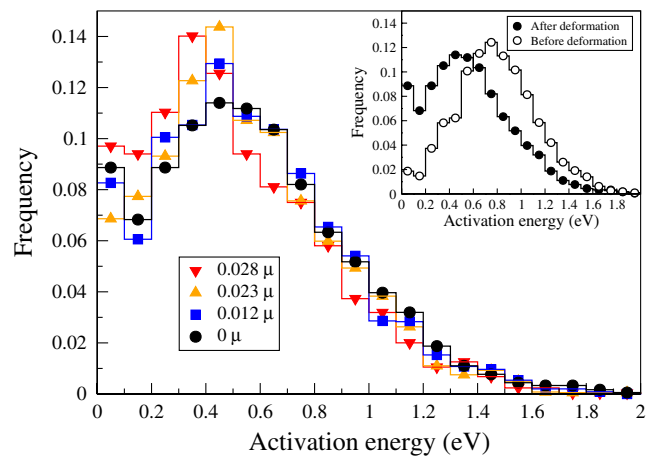


FIG. 2 (color online). Frequency of activation energies in configurations issued from a given unloading at different shear stresses noted on the figure. Frequencies were obtained after binarization (bin size 0.1 eV) of the data collected from 4000 different events. The inset shows the distributions in the glass before plastic deformation (open circles) and in the unloaded configuration after plastic deformation (filled black circles, from the configuration at 0μ in the main frame).

states in our simulations. On the other hand, many states loosely exhibit a quadrupolar symmetry as in Fig. 1, or no discernible symmetry at all.

We first consider the distribution of activation energies in flowing glass and its dependence upon the applied stress (assessed during elastic unloading). Figure 2 shows such distributions for four configurations with different average shear stresses ranging from very high (downward triangles, taken directly from the flow state of the quasistatic shear simulation) down to zero (circles, corresponding to the unloaded state). The elastic unloading has no significant effect on the distributions that all exhibit a similar wide shape, extending from 0 to 2 eV with a maximum at around 0.4 eV. The inset in Fig. 2 compares the distributions in the glass before and after quasistatic plastic deformation. We see that the plastic deformation has created a large fraction of low-energy barriers, implying that during deformation the glass has adopted a microstructure of higher energy and lower stability than the initial undeformed configuration.

The shape of the distributions in Fig. 2 is characteristic of a complex energy landscape as expected for atomistic processes in an amorphous solid [19]. Similar distributions have been extracted from relaxation simulations at finite temperature [9], and the few existing efforts to back out such distribution from experiments in creep condition [22,23] also reveal a shape comparable to that shown in Fig. 2, but with negligibly few low-energy barriers. Deformed experimental glasses are more stable because they are deformed at lower stresses and undergo thermally activated relaxation during the deformation process.

We now turn our attention to the distributions of plastic strains between initial and final configurations, which are shown in Fig. 3 for the same configurations as in Fig. 2. The strain distributions in Fig. 3 are broad, contain negative strain events, and exhibit maxima at finite strains, including the distribution computed from the high-stress configuration taken from the quasistatic simulation (downward triangles). This result deviates substantially from the ana-

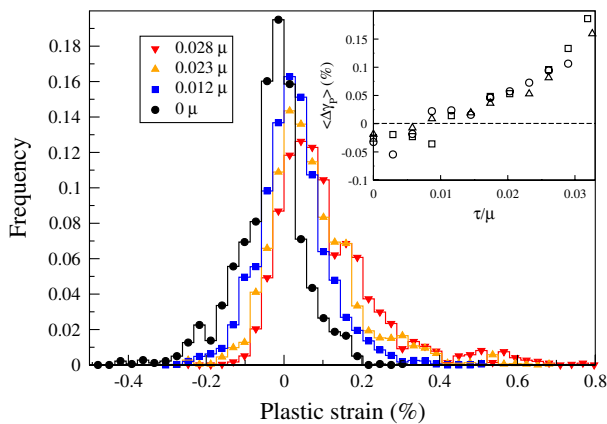


FIG. 3 (color online). Frequency of plastic strains in the same configurations as in Fig. 2 (bin size $3 \times 10^{-4} \mu$). The inset shows the average plastic strain as a function of stress for 3 unloadings.

log distribution computed from the succession of plastic events during quasistatic deformation, which exhibits only positive strain events and decreases exponentially with strain [13]. Its only maximum is therefore asymptotic at zero strain. We conclude, then, that the subset of plastic events sampled by quasistatic simulations is biased towards small strain events and is not representative of the distribution of thermally activated events in the glass. At lower stress levels below mechanical instability, the distributions shift towards zero plastic strain, a consequence of the decrease in stress bias.

The inset in Fig. 3 shows the average plastic strain computed from the above distributions as a function of shear stress for different unloadings. The dependence is approximately linear, and interestingly, the average strain is systematically negative after unloading. This effect is also visible in the strain distribution at zero stress (circles), which is asymmetrical and skewed towards negative events. This is a signature of the polarization of the flow state [23] acquired by the accumulation of positive strain events during the initial quasistatic deformation. Relaxation of the flow state at finite temperature will decrease the polarization by involving more negative than positive events, leading to creep recovery, i.e., a relaxation of the system shape towards its initial shape [23]. A polarized flow state is also at the origin of the Bauschinger effect evidenced in Refs. [6,9].

We now show that there is no significant correlation between the activation energy of an event and its associated plastic strain. This conclusion is based on Fig. 4, which presents, as a function of activation energy, the plastic strains in both the final and activated states of the 4000 events determined on the high-stress configuration considered above. For each activation energy, there is a broad distribution of associated plastic strains, both in the activated and final configurations. Note, however, that there is

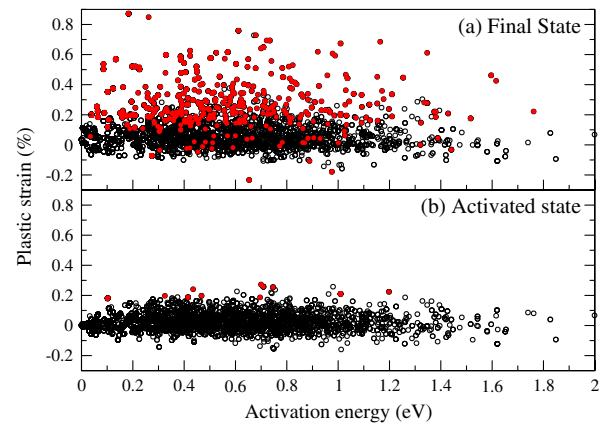


FIG. 4 (color online). Plastic strain in the (a) final and (b) activated states as a function of activation energy for the 4000 events determined on the high-stress configuration of Figs. 2 and 3 ($\tau = 0.033\mu$). In gray (red) are the events that percolate through the simulation cell (see text for details).

a slight tendency for low- and high-energy events to produce smaller strains. These observations are consistent at all stress levels.

The morphology of the plastic events may be characterized by the size of the atomic clusters involved in the rearrangements, and whether these clusters percolate through the simulation cell. The clusters were determined for each event by building the cluster of atoms linked by first-neighbor bonds and displaced by more than 0.1 Å, starting from the most displaced atom. Events with a cluster that percolates through the simulation cell are shown in gray (red) in Fig. 4, where we see that, remarkably, either localized or percolating events can be seen in the final configuration [Fig. 4(a)] at any activation energy; percolation is not associated exclusively with higher energy events. On the other hand, there is a threshold in strain: few events with a plastic strain less than about 0.1% are localized, while above this value, most events percolate. While the position of the threshold depends on the reference value chosen to identify displaced atoms, its existence does not.

Finally, Fig. 4(b) shows that the spectrum of plastic strains in the activation state is narrower than in the final configuration. Most activated states are made of localized clusters, which are more likely because of the localized nature of thermal fluctuation. Nonetheless some events still percolate through the simulation cell.

In conclusion, we have used ART to explore the energy landscape of a plastically deformed glass. The flow state is shown to be strongly influenced by the plastic deformation with characteristic distributions that contain a large fraction of low-energy barriers due to the system's marginal stability, and a larger fraction of negative strain events due to its polarization by the applied positive shear strain. These results underscore the highly nonequilibrium flow state attained in quasistatic simulations, and call for the development of new complementary modeling approaches for amorphous systems.

The authors would like to thank Professor A. S. Argon for insightful discussions on plasticity in amorphous solids and Dr. C. Marinica for pointing out the work in Ref. [20]. This work was funded by the Délégation Générale à

l'Armement. C. S. acknowledges support from the U.S. Office of Naval Research under Contract No. N00014-08-1-0312.

*On sabbatical leave from the Institut Polytechnique de Grenoble, France.

- [1] C. A. Schuh, T. C. Hufnagel, and U. Ramamurty, *Acta Mater.* **55**, 4067 (2007).
- [2] M. J. Demkowicz and A. S. Argon, *Phys. Rev. Lett.* **93**, 025505 (2004).
- [3] D. Rodney, M. Fivel, and R. Dendievel, *Phys. Rev. Lett.* **95**, 108004 (2005).
- [4] F. Varnik, L. Bocquet, J. L. Barrat, and L. Berthier, *Phys. Rev. Lett.* **90**, 095702 (2003).
- [5] Y. Shi and M. L. Falk, *Phys. Rev. Lett.* **95**, 095502 (2005).
- [6] M. L. Falk and J. S. Langer, *Phys. Rev. E* **57**, 7192 (1998).
- [7] J. S. Langer, *Phys. Rev. E* **77**, 021502 (2008).
- [8] S. Kobayashi, K. Maeda, and S. Takeuchi, *Acta Metall.* **28**, 1641 (1980).
- [9] D. Deng, A. S. Argon, and S. Yip, *Phil. Trans. R. Soc. A* **329**, 549 (1989).
- [10] F. H. Stillinger and T. A. Weber, *Science* **225**, 983 (1984).
- [11] D. L. Malandro and D. J. Lacks, *Phys. Rev. Lett.* **81**, 5576 (1998).
- [12] A. S. Argon, *Acta Metall.* **27**, 47 (1979).
- [13] C. E. Maloney and A. Lemaître, *Phys. Rev. Lett.* **93**, 016001 (2004).
- [14] A. Tanguy, F. Leonforte, and J. L. Barrat, *Eur. Phys. J. E* **20**, 355 (2006).
- [15] M. J. Demkowicz and A. S. Argon, *Phys. Rev. B* **72**, 245206 (2005).
- [16] S. G. Mayr, *Phys. Rev. Lett.* **97**, 195501 (2006).
- [17] F. Delogu, *Phys. Rev. Lett.* **100**, 255901 (2008).
- [18] R. Malek and N. Mousseau, *Phys. Rev. E* **62**, 7723 (2000).
- [19] F. Valiquette and N. Mousseau, *Phys. Rev. B* **68**, 125209 (2003).
- [20] E. Cancès, F. Legoll, M. C. Marinica, K. Minoukadeh, and F. Willaime, *J. Chem. Phys.* **130**, 114711 (2009).
- [21] A. W. Lees and S. F. Edwards, *J. Phys. C* **5**, 1921 (1972).
- [22] D. Deng and A. S. Argon, *Acta Metall.* **34**, 2025 (1986).
- [23] A. S. Argon and H. Y. Kuo, *J. Non-Cryst. Solids* **37**, 241 (1980).